

Full Length Research Paper

Assessing future changes in extremes precipitations indices in Ouémé River basin at Bétérou (Benin, West Africa)

Biao Iboukoun Eliézer^{1, 2*}, Obada Ezéchiel² and Alamou Adéchina Eric²

¹National School of Mathematical Engineering and Modeling, National University of Sciences, Technology, Engineering and Mathematics, Abomey, Benin.

²LaGEA, National School of Public Works, National University of Sciences, Technology, Engineering and Mathematics, Abomey, Benin.

Received 5 March, 2024; Accepted 29 April 2024

Understanding changes in precipitation intensity and frequency indices plays an important role in flood risk mitigation and water resource management. The objective of this paper is to assess future changes in extreme precipitation indices in the Oueme River basin at Bétérou compared to the reference period. To achieve this, the paper uses the ISIMIP approach to improve the usability of regional climate model projections for climate change impact studies. This impact study evaluates changes in some of the extreme climate indices recommended by the Expert Team Monitoring on Climate Change Detection and Indices. The bias correction approach helps to reduce differences between observed rainfall and the precipitation data from regional climate models (HIRHAM5, REMO, and RCA4). For future projections, the results indicate a mix of increases and decreases in precipitation intensity indices (simple daily intensity index and Max 5-day precipitation amount), ranging between -40 and 40% with HIRHAM5 and RCA4, while with REMO, only increases ranging between 2 and 80% are simulated under both RCP4.5 and RCP8.5 scenarios across the three time horizons: 2020s (2011–2040), 2050s (2041–2070), and 2080s (2071–2100), representing the near, mid, and far future. Regarding precipitation frequency indices (number of heavy precipitation events, number of very heavy precipitation events, consecutive dry days, and consecutive wet days), the results also show a mix of increases and decreases, ranging between -40 and 80%, over the three time horizons under both RCP4.5 and RCP8.5 scenarios using HIRHAM5, REMO, and RCA4 precipitation data.

Key words: Extremes precipitations indices, future projection, regional climate models, ISIMIP method, Ouémé River.

INTRODUCTION

Recent decades have witnessed increasing concern among the international scientific community about climate change and its impacts on extreme climates. The

Intergovernmental Panel on Climate Change (IPCC) has noted a widespread viewpoint among climate scientists that events such as droughts and floods, now regarded

*Corresponding author. E-mail: biaoeliezer@yahoo.fr

as extremes, are projected to become more frequent and widespread in the future (IPCC, 2014). From the perspective of climate change impacts, the most noticeable and heavily felt are the extreme weather and climate events because of their immediate and disastrous consequences on the natural and social environment (Ahsan et al., 2021). Moreover, several studies (Orlowsky and Seneviratne 2012; Kharin et al., 2013; Sillmann et al., 2013) have projected the changing patterns of extreme climate events along with rising anthropogenic greenhouse gas emissions.

Extreme precipitation is projected to increase significantly, especially in regions that are already relatively wet under present climate conditions, whereas dry spells are predicted to increase particularly in regions characterized by dry conditions in the present-day climate (Christensen et al., 2007; Sillmann and Roeckner, 2008). Extreme precipitation events have been usually investigated using the Expert Team on Climate Change Detection and Indices (ETCCDI) (Zhang et al., 2011). These indices describe particular characteristics of extremes, including frequency, amplitude, and persistence. Several researchers worldwide have used the ETCCDI climate indices to analyze possible changes in extreme precipitation events over the past (Donat et al., 2016; Lacovone et al., 2020; Ceron et al., 2021; Regoto et al., 2021; Faye and Akinsanola, 2022; Alechy et al., 2022) and for future climates using climate model projections (Thibeault and Seth, 2014; Xu et al., 2019; Avila-Diaz et al., 2020; Gouveia et al., 2022; Paul and Maity, 2023).

West Africa is particularly vulnerable to climate change due to its high climate variability, its high reliance on rain-fed agriculture, and its limited economic and institutional capacity to respond to climate variability and change (Sultan and Gaetani, 2016). In the recent past, the assessment of climate change in West Africa was made with the outputs of the Global Climate Model (GCM) (IPCC, 2007). With a grid ranging from 150 to 400 km², GCMs have great difficulties in taking into account regional heterogeneities of variability and changes in climate. This means that these models are not suitable for producing climate projections at the regional, national, and local scales, which are necessary to assess the impacts of climate change and to develop adaptation policies (Paeth, 2011). Faced with this situation, projects such as AMMA (African Monsoon Multidisciplinary Analyses), ENSEMBLE (a project that produced a multi-model ensemble at approximately 25 km resolution), and CORDEX AFRICA (Coordinated Regional Climate Downscaling Experiment) have been developed to produce variables at the regional scale. Regional Climate Models (RCMs) were therefore forced by GCM outputs in the West Africa region with a spatial resolution of 50 km. To date, relatively few studies have assessed the impacts of climate change on extreme precipitation indices, and a clear picture of possible changes is lacking in the Oueme River basin at the Beterou catchment. In order to fill this

gap, this study assesses the impacts of climate change on extreme precipitation indices by using bias-corrected data from three Regional Climate Models (DMI-HIRHAM5, SMHI-RCA4, and MPI-REMO) simulations. These corrected data are used to compute the extreme precipitation indices for the analysis of changes in future extreme precipitation indices.

MATERIALS AND METHODS

In West Africa, the Ouémé River is a small coastal river that extends to Bonou, the most advanced hydrological station before the delta, covering an area of 46,990 km². It is the largest river in Benin, originating from the classified forest of Tanéka (Atacora) (Le Lay, 2006). This river alone covers more than a third of the territory of Benin. The Ouémé River basin at the Bétérou outlet is located between 09°12'N latitude and 02°16'E longitude, covering an area of 14,000 km² (Figure 1). This basin lies in the Sudanese savanna zone and experiences a unimodal rainfall season from mid-March to October, peaking in August. The interannual mean rainfall on the Ouémé at Bétérou is approximately 1160 mm, with a minimum of 743 mm (recorded in 1983) and a maximum of 1587 mm (recorded in 1963) over the period 1961-2010 (Lawin, 2007). The river's discharge dynamics are characterized by high flow during the rainy season, while from December to May, nearly all rivers dry out.

Observed daily precipitation data were provided by the Benin Meteorological Department, that is, Météo-Bénin, for the period 1961-1990. Historical and future projections (under RCP4.5 and RCP8.5 scenarios) of precipitation data from three regional climate models (SMHI-RCA4, DMI-HIRHAM5, MPI-REMO) were obtained from the CORDEX Africa project (<http://www.cordex.org>). These three RCMs were selected to assess their ability to replicate observed precipitation data in the Oueme catchment at Beterou outlet for impact studies. The reference period chosen to examine bias in precipitation is the period 1961-1990 (baseline period), which is considered the World Meteorological Organization (WMO) standard normal period.

For future projections, the RCP4.5 (moderate emissions scenario) and RCP8.5 (high emissions scenario) scenarios are considered over the period 2011-2100. RCP4.5 represents a stabilization scenario, chosen because it somewhat reflects the medium-low RCP (representative concentration pathways). In contrast, RCP8.5 reflects the impact of the largest potential climate change due to increasing greenhouse gas emissions. The baseline period 1961-1990 was used to represent the 'present-day' climatology of the study area. Climate scenarios were centered around three timeframes: 2020s (2011-2040), 2050s (2041-2070), and 2080s (2071-2100), representing the early, middle, and late 21st century, respectively.

The HIRHAM5, RCA4, and REMO simulations were forced with data from the global climate models GFDL-ESMLM, EC-EARTH, and MPI-ESM-LR (Table 1). The entire simulated period spans from 1951 to 2100, with the first 54 years (historical: 1951-2005) representing the historical period. The remaining period (2006-2100) was forced by the RCP scenarios RCP4.5 and RCP8.5.

The present study utilized 6 ETCCDI indices (Table 2). These selected indices not only capture the intensity and duration of changes in precipitation but also the frequency and length of heavy precipitation events (Alamou et al., 2022). They enable us to assess the spatial and temporal distribution of extreme events in the study area. All investigated extreme precipitation indices are calculated from daily precipitation data.

Due to the well-known bias of climate model output, a bias correction technique is applied to correct the simulations of the three RCMs (DMI-HIRHAM5, SMHI-RCA4, and MPI-REMO) for the

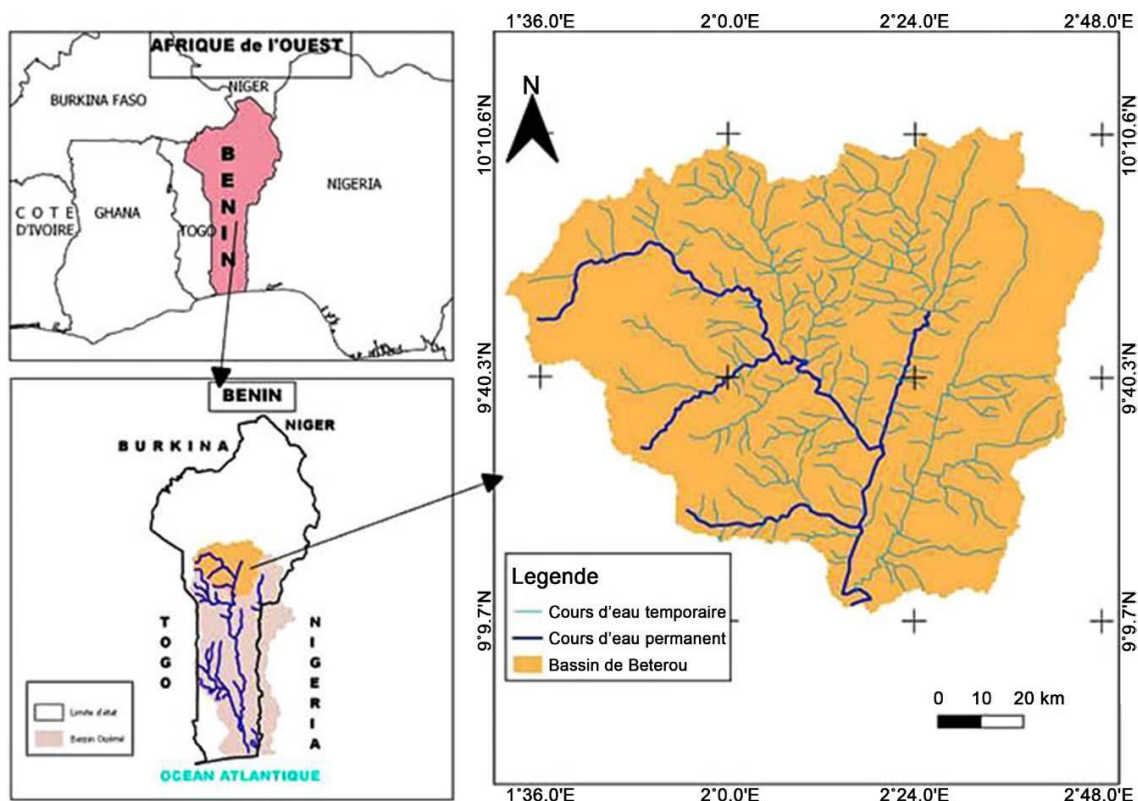


Figure 1. Study area.

Table 1. Main characteristics of the RCM used.

| RCM | Institution | Driving GCM | Horizontal Resolution (km) | No. of vertical levels | Simulation period | References |
|---------|-------------|-------------|----------------------------|------------------------|-------------------|---------------------------|
| HIRHAM5 | DMI | GFDL-ESMLM | 50 | 31 | 1951-2100 | Christensen et al. (2017) |
| RCA4 | CSC | EC-EARTH | 50 | 40 | 1951-2100 | Jacob et al. (2007) |
| REMO | SMHI | MPI-ESM-LR | 50 | 27 | 1951-2100 | Samuelsson et al. (2011) |

present day and future climate. Bias correction removes errors resulting from the large spatial scale of grid cells in models that do not account for local climate specificity. In this study, the ISIMIP bias correction method is applied to improve the usability of regional climate model projections for climate change impact studies (Yang et al., 2010; Haylock et al., 2006). The Root Mean Square Error (RMSE) and Mean Absolute Error (MAE) performance criteria are used to evaluate the bias correction method's effectiveness on precipitation data.

To assess the impact of climate change on extreme precipitation indices, the rate of mean precipitation indice variations has been computed. The spatial pattern of this rate allows us to contrast changes in the future under RCP4.5 and RCP8.5 scenarios compared to the reference period (Equation 1):

$$\text{Rate of variation} = \frac{X_{\text{future}} - X_{\text{reference}}}{X_{\text{reference}}} \times 100 \quad (1)$$

where X_{future} represents the bias corrected projected extreme

precipitation indices from the RCP4.5 and RCP8.5 scenarios over the 2020s (2011 - 2040), 2050s (2041-2070), and 2080s (2071-2100), and $X_{\text{reference}}$ represents the reference period. Linear trends were calculated for each investigated precipitation index to explore the variability in the magnitude of indices under a changing climate during the various spans of the twenty-first century. The magnitude of the trend was calculated using Sen's (1968) slope estimator, and the statistical significance of trends was established using Mann-Kendall's tau test at confidence levels of 95%. The trends were calculated for the near future (2011-2040), mid-future (2041-2070), and far future (2071-2100).

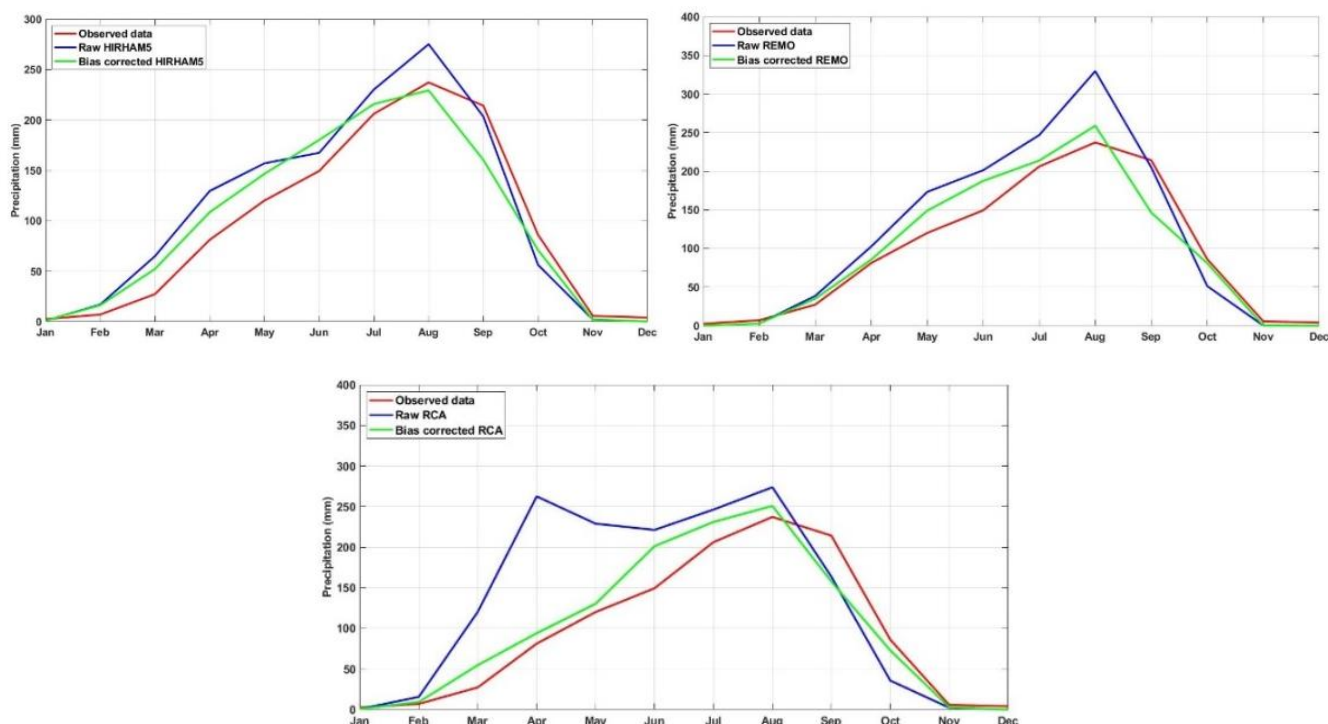
RESULTS

Evaluation of the ISIMIP bias correction

The ISIMIP method resulted in a more realistic representation of local climate compared to using raw RCM output. After applying the ISIMIP bias correction,

Table 2 Precipitations indices summary.

| Common name | Indices | Description | Units |
|------------------------------------|---------|--|---------|
| Number of heavy precipitation | R10 | Annual count of days when PRCP \geq 10 mm | days |
| Number of very heavy precipitation | R20 | Annual count of days when PRCP \geq 20 mm | days |
| Consecutive dry days | CDD | Maximum number of consecutive days with RR<1 mm | days |
| Consecutive wet days | CWD | Maximum number of consecutive days with RR \geq 1 mm | days |
| Simple daily intensity index | SDII | Annual total precipitation divided by the number of wet days (defined as PRCP \geq 1.0 mm) in the year | mm/days |
| Max 5-day precipitation amount | RX5day | Annual maximum consecutive 5-day precipitation | mm |

**Figure 2.** ISIMIP bias correction for HIRHAM5, RCA4 and REMO precipitation data over the reference period 1961 – 1990.

the substantial differences between the observations and simulations were considerably reduced. Figure 2 illustrates the outcomes of applying the ISIMIP method to the three investigated RCMs in the B  terou catchment. It is evident from this figure that the bias-corrected data closely resemble the observed data compared to the raw RCM data.

To further assess the effectiveness of the bias correction, parameters such as the Root Mean Square Error (RMSE) and the Mean Absolute Error (MAE) are examined. The performance statistics for comparing observed monthly precipitations, raw monthly HIRHAM5 precipitations, corrected monthly HIRHAM5, raw monthly RCA4 precipitations, and corrected monthly RCA4 precipitations are presented in Table 3. The results of the

bias correction indicate a decrease in the RMSE (9.91% for the raw HIRHAM5, 34.53% for the raw REMO, 65.58% for the raw RCA4 precipitation data) and a decrease in the MAE (18.29% for the raw HIRHAM5, 40.44% for the raw REMO, 6.6% for the raw RCA4 precipitation data).

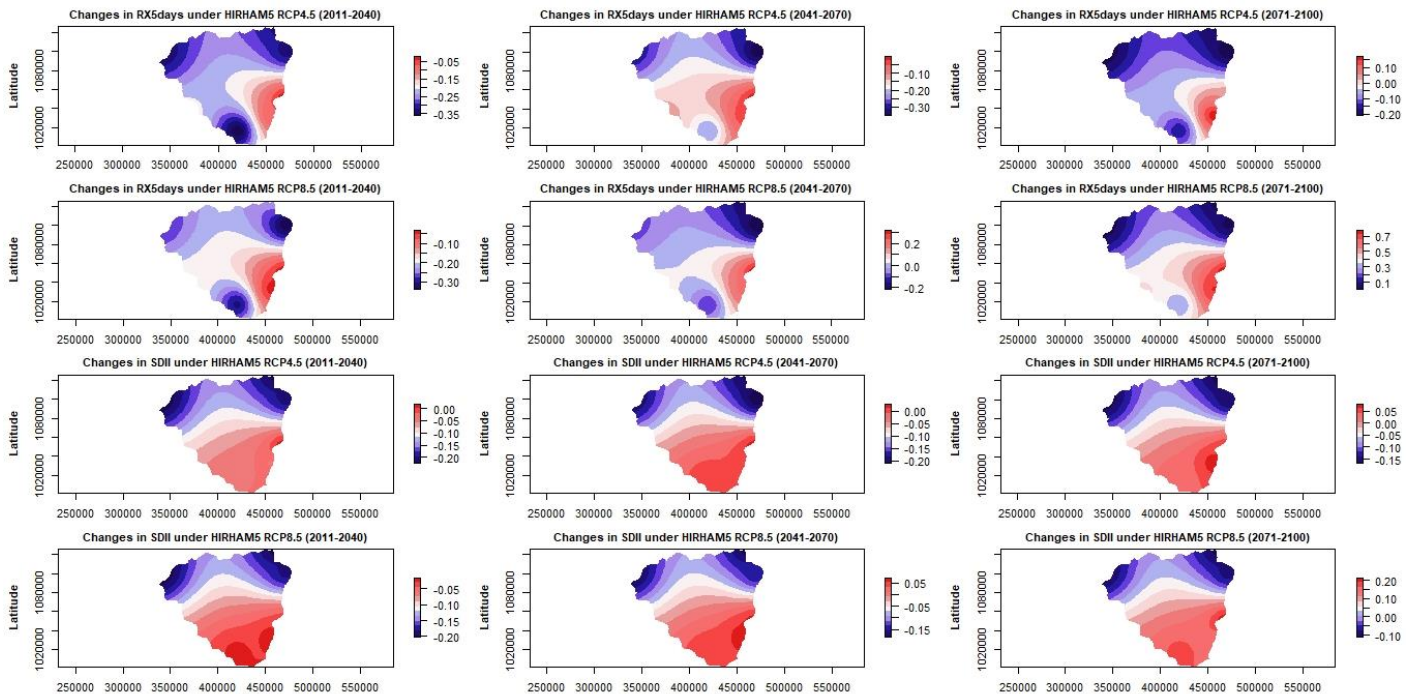
Changes in precipitations intensity indices (RX5day, SDII)

Changes in precipitations intensity indices using HIRHAM5 precipitations data

Figure 3 shows changes in RX5day and SDII over the near, mid and far future under RCP4.5 and RCP8.5

Table 3. Performance statistics comparing observed monthly rainfall, raw monthly RCM precipitations and bias corrected monthly RCM precipitations.

| Performances criteria (mm/month) | Raw HIRHAM5 | Bias corrected HIRHAM5 | Raw REMO | Bias corrected REMO | Raw RCA4 | Bias corrected RC4 |
|----------------------------------|-------------|------------------------|----------|---------------------|----------|--------------------|
| RMSE | 26.77 | 23.12 | 38.34 | 25.10 | 74.52 | 25.65 |
| MAE | 21.87 | 17.87 | 27.57 | 16.42 | 54.18 | 18.42 |

**Figure 3.** Changes in RX5days and SDII using HIRHAM5 precipitations data.

scenarios compared to the reference period. Under RCP4.5 scenarios, most of the regions of the study area would experience a decrease in RX5days. The decrease in RX5days ranges between 5 and 40% in the near and mid future. However, an increase ranging between 5 and 15% is observed in the south-east of Beterou catchment in the far future. Under RCP8.5 scenarios, a decrease ranging between 5 and 30% would be noticed in the near future, while an increase of about 10 to 70% is simulated in the mid and far future. Under RCP4.5 scenarios, the study area would experience a decrease in SDII ranging between 5 and 20% over the three sub-periods. Under RCP8.5 scenarios, a decrease of approximately 5 to 20% is simulated in the near future, whereas in the mid and far future an increase up to 20% could be observed in the south.

Changes in precipitations intensity indices using REMO precipitation data

Figure 4 shows changes in RX5day and SDII by using REMO precipitations simulations over the near, mid and

far future under RCP4.5 and RCP8.5 scenarios compared to the reference period. Under RCP4.5 scenarios, all the study area would experience an increase in RX5days. The highest increase (up to 90%) could be observed in the north, while the smallest increases, ranging between 20 and 40% are simulated in the south and in the north-east over the three sub-periods. Under RCP8.5 scenarios, the same conclusion can be drawn in the north and in the south. The highest increase in the north is around 70% and the smallest increase in the south is found to be 30%.

Under RCP4.5 scenarios, the study area would also experience an increase in SDII ranging between 1 and 30% over the three sub-periods. The highest increase is simulated in the south over the period 2041 - 2070. Under RCP8.5 scenarios, a slight increase (2 to 14%) in SDII can be noticed over the investigated sub-periods.

Changes in precipitations intensity indices using RCA4 precipitations data

Figure 5 shows changes in RX5day and SDII by using

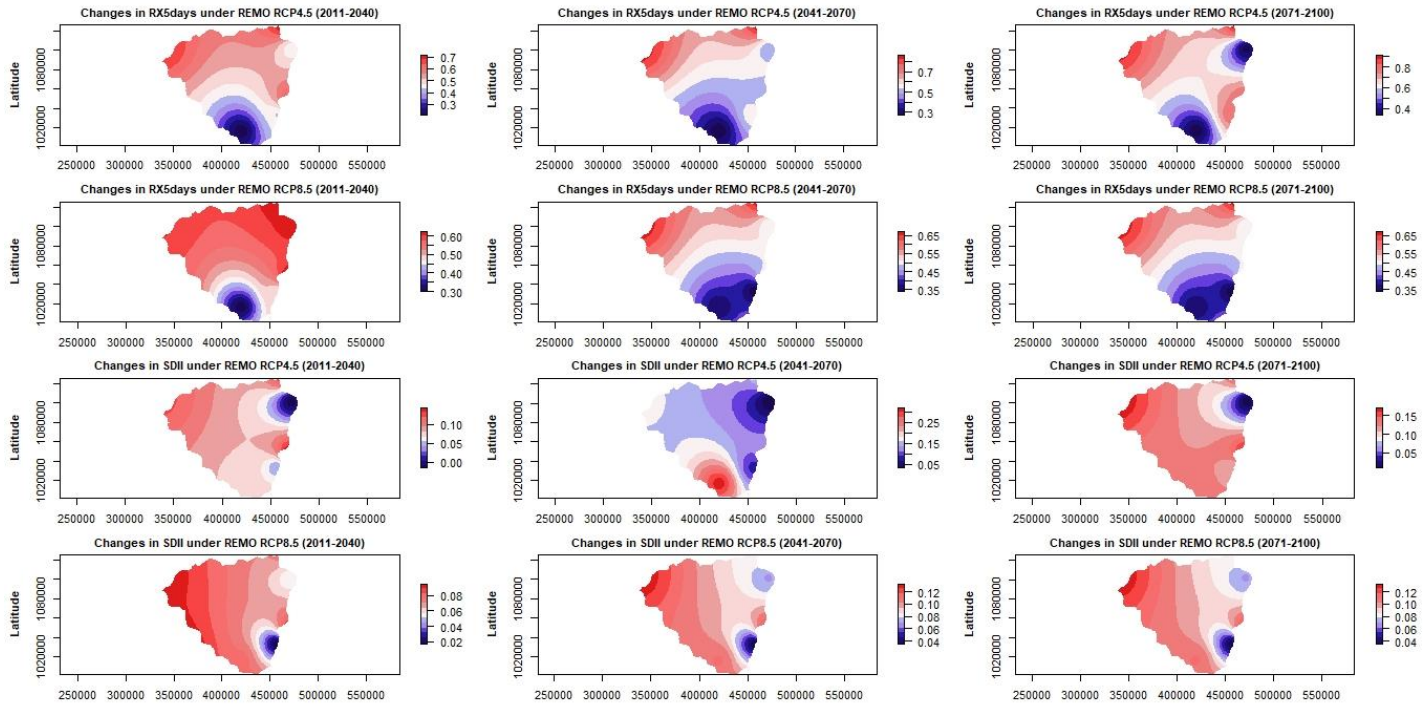


Figure 4. Changes in RX5days and SDII using REMO precipitations data.

RCA4 precipitations simulations over the near, mid and far future under RCP4.5 and RCP8.5 scenarios compared to the reference period. Under RCP4.5 and RCP8.5 scenarios, a mix of increase (up to 40%) and a decrease (up to 20%) in RX5days is simulated over the sub-periods. The increase is found in the south-east. Regarding SDII, we also simulated a mix of increase (up to 15%) and a decrease (up to 10%) respectively in the south and in the north. The highest decrease is found in the north-west.

Projected changes in annual precipitations intensity indices over the near, mid and far future under RCP4.5 and RCP8.5 scenarios

Figure 6 shows changes in annual RX5days and SDII under RCP 4.5 and RCP 8.5 scenarios and for the different investigated RCM precipitations. It can be seen that projected changes in annual RX5days using HIRHAM5, REMO and RCA4 precipitations simulations under RCP4.5 and RCP8.5 scenarios are different. Indeed, RX5days shows a decrease of 18% (2020s), 10% (2050s) and 2% (2080s) under RCP4.5 scenarios, while under RCP8.5 scenarios it will be observed a decrease of 15% (2020s), an increase of 5% (2050s) and 40% (2080s) with HIRHAM5 simulations. Regarding REMO simulations, RX5days shows an increase of 55% (2020s), 58% (2050s) and 68% (2080s) under RCP4.5 scenarios, while under RCP8.5 scenarios an increase of

60% (2020s), 56% (2050 and 2080s) could be observed. With RCA4 simulations, RX5days shows an increase of 12% (2020s), 10% (2050s) and 8% (2080s) under RCP4.5 scenarios, while under RCP8.5 scenarios an increase of 2% (2020s), 7% (2050s) and 8% (2080s) could be observed. SDII shows a decrease of 7% (2020s), 5% (2050s) and 1% (2080s) under RCP4.5 scenarios, while under RCP8.5 scenarios a decrease of 7% (2020s) and 1% (2050s) will be observed and an increase of 9% (2080s) with HIRHAM5 simulations. Regarding REMO simulations, SDII shows an increase of 10% (2020s), 12% (2050s) and 12.5% (2080s) under RCP4.5 scenarios, while under RCP8.5 scenarios an increase of 10% (2020s), 12% (2050s and 2080s) could be observed. With RCA4 simulations, SDII shows an increase of 7.5% (2020s), 2% (2050s) and 4% (2080s) under RCP4.5 scenarios, while under RCP8.5 scenarios an increase of 2% (2020s), 2.5% (2050s) and 4% (2080s) could be observed.

Changes in precipitations frequency indices (R10, R20, CDD, CWD)

Changes in precipitation frequency indices using HIRHAM5 precipitations data

Changes in R10 and R20 by using HIRHAM5 precipitations simulations over the near, mid and far future under RCP4.5 and RCP8.5 scenarios compared to

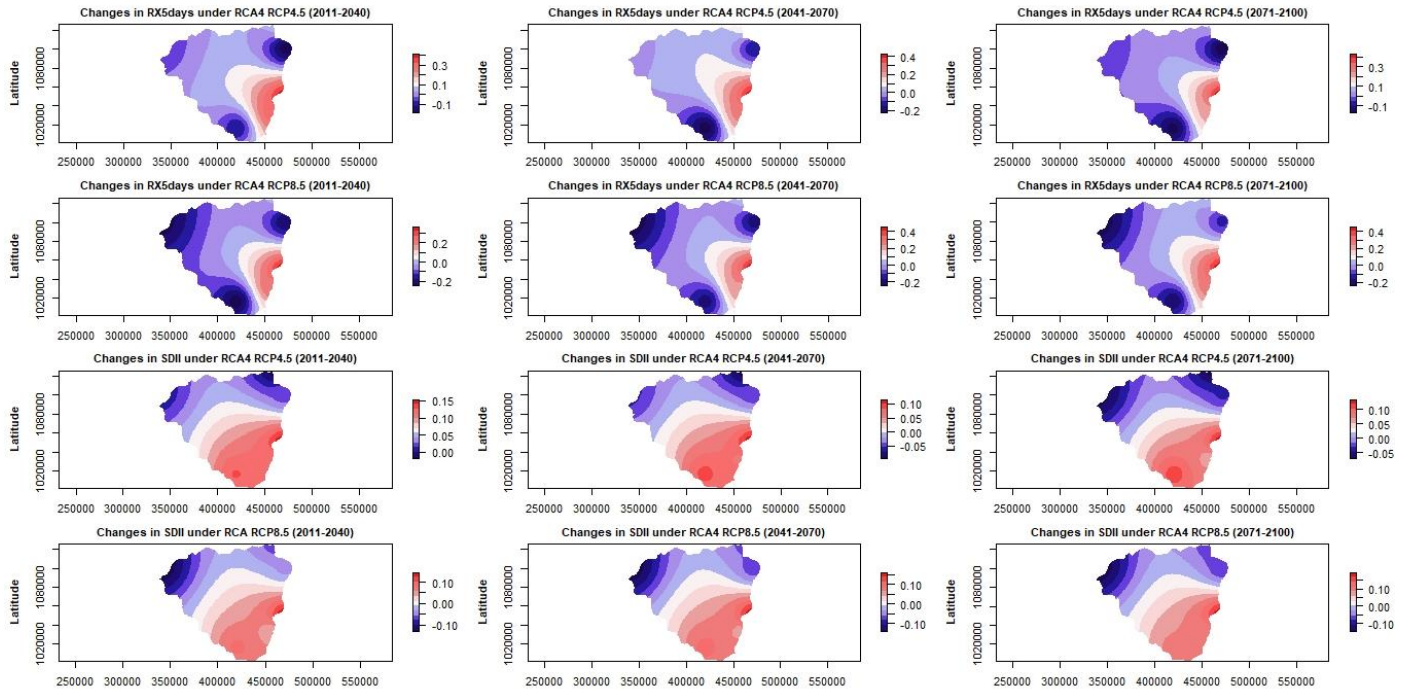


Figure 5. Changes in RX5days and SDII using RCA4 precipitations data.

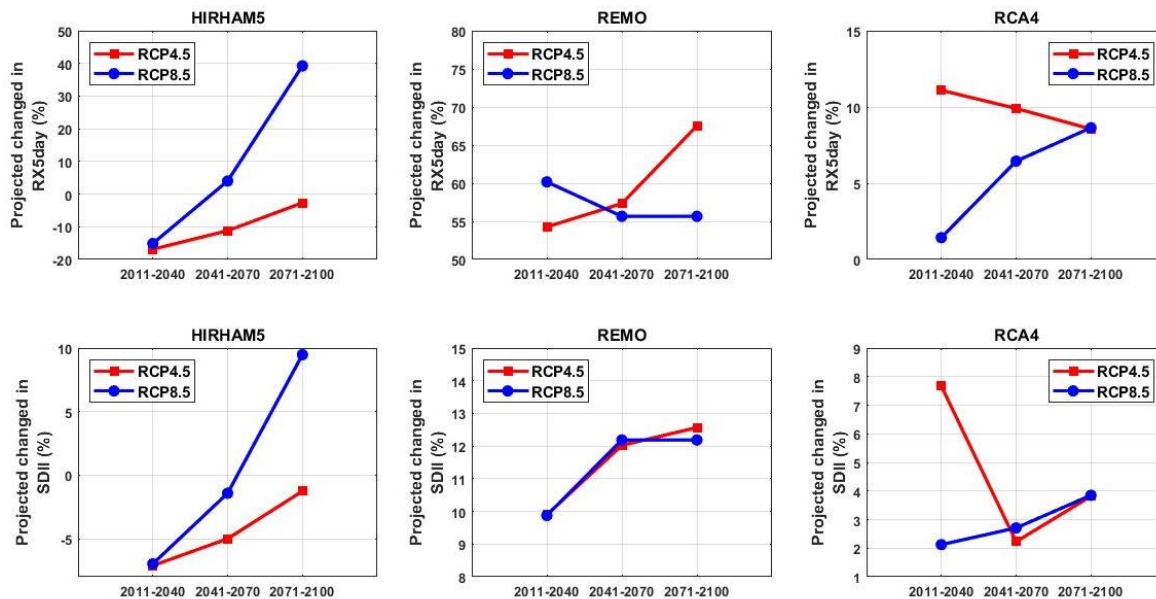


Figure 6. Projected changes in annual RX5days and SDII under RCP 4.5 and RCP 8.5 scenarios.

the reference period are shown in Figure 7. Under RCP4.5 and RCP8.5, the same pattern of R10 is simulated over the three sub-periods. An increase in R10 ranging between 30 and 80% can be observed in the study area. The highest increase is found in the south-east. Under RCP4.5 and RCP8.5 scenarios, most of the region shows

a decrease in R20 (up to 60%) over the sub-periods. However, an increase in R20 (up to 25%) is simulated in the south-east for the far future.

Figure 8 shows changes in CDD and CWD over the near, mid and far future under RCP4.5 and RCP8.5 scenarios compared to the reference period. Under RCP4.5

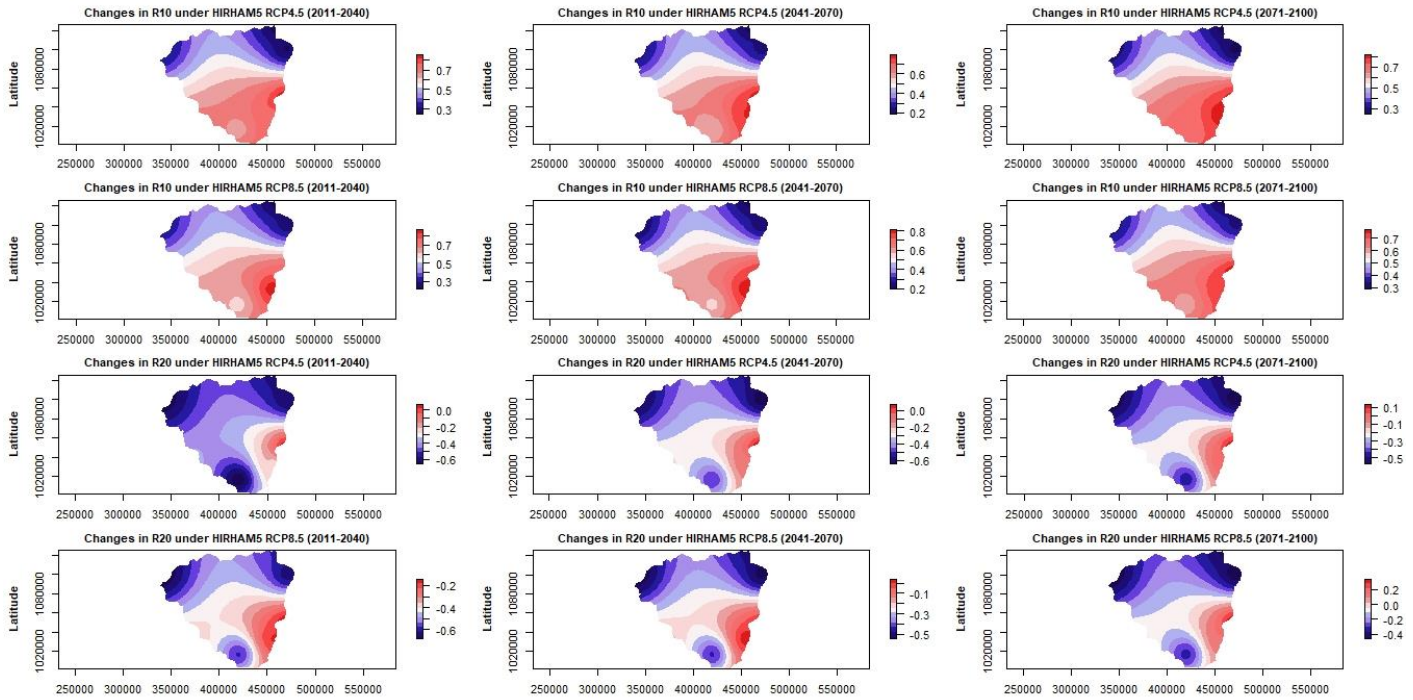


Figure 7. Changes in R10 and R20 using HIRHAM5 precipitations data.

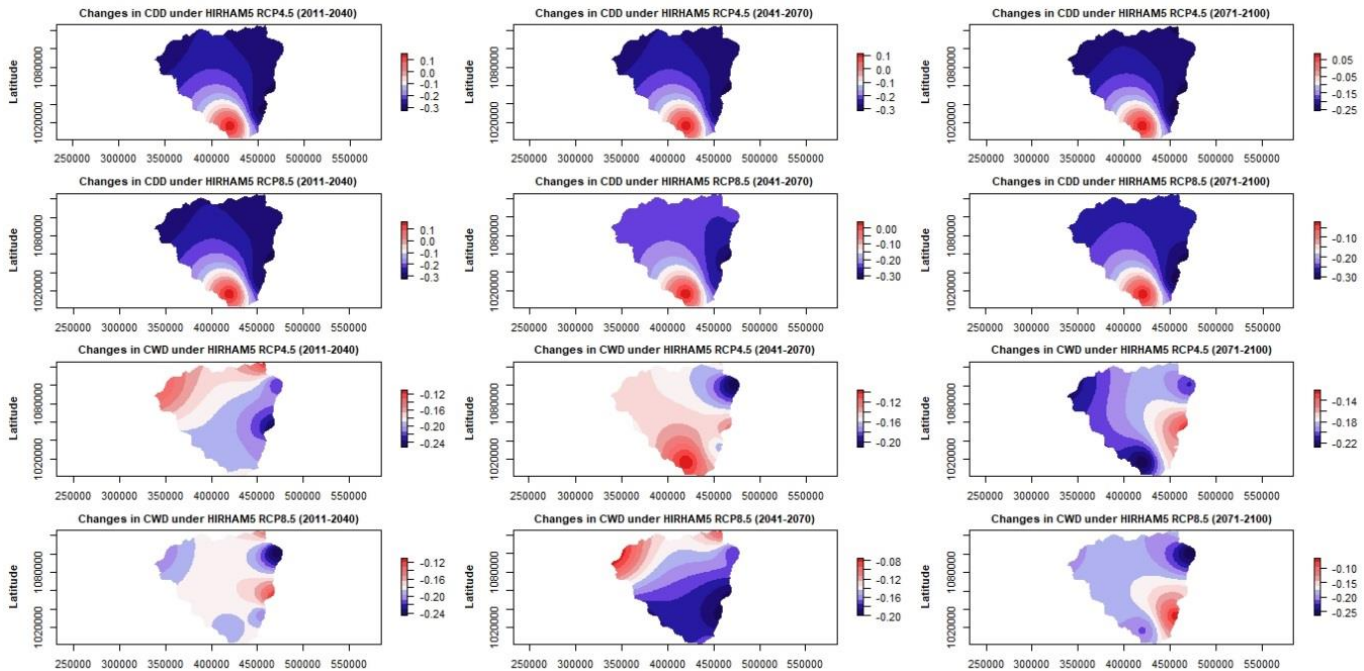


Figure 8. Changes in CDD and CWD using HIRHAM5 precipitations data.

and RCP8.5, most of the region would experience a decrease in CDD (up to 30%) over the three sub-periods, except the south-east where an increase up to 25% can be

found. Under RCP4.5 and RCP8.5, a decrease in CWD ranging between 8 and 25% is simulated through the area over the near, mid and far future.

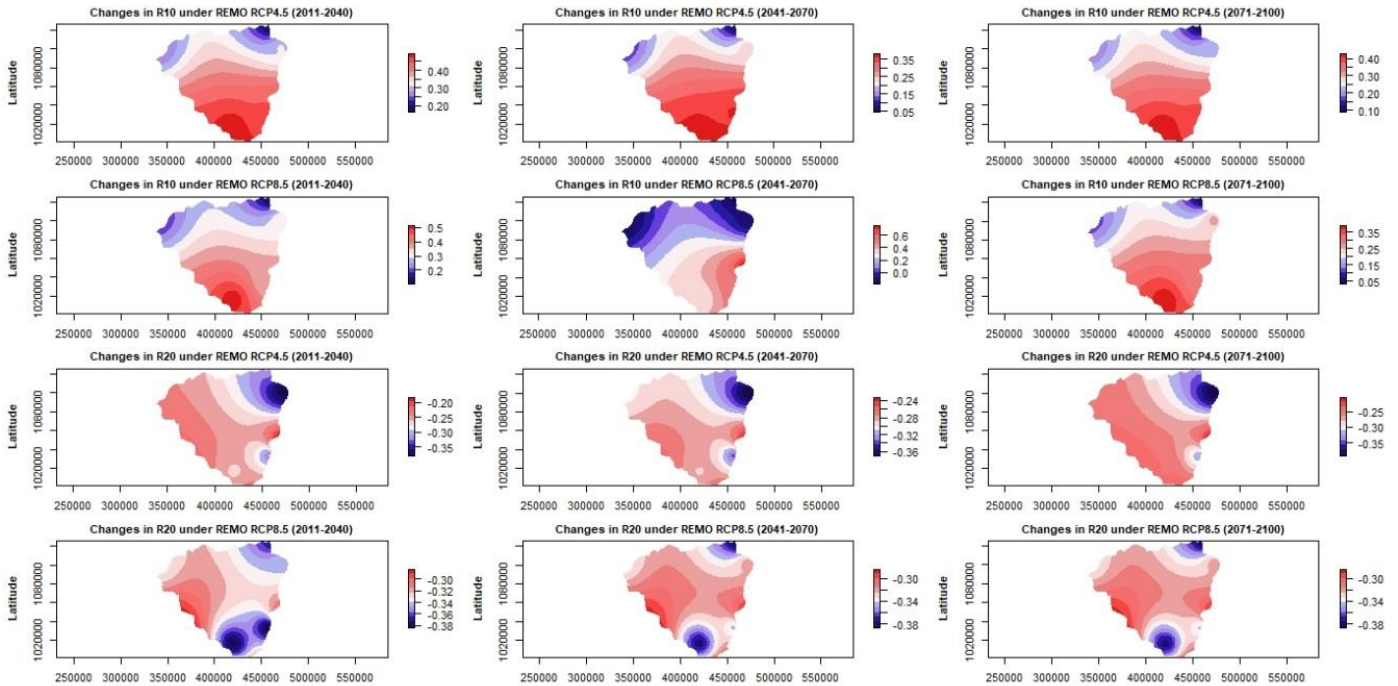


Figure 9. Changes in R10 and R20 using REMO precipitations data.

Changes in precipitations frequency indices using REMO precipitations data

Changes in R10 and R20 by using REMO precipitations simulations over the near, mid and far future under RCP4.5 and RCP8.5 scenarios compared to the reference period are shown in Figure 9. Under both RCP4.5 and RCP8.5 scenarios, an increase in R10 ranging between 5 and 65% is simulated over the three sub-periods. The highest increase is found mostly in the south. Under RCP4.5 and RCP8.5 scenarios, most of the region show a decrease in R20, ranging between 20 and 40% over the sub-periods.

Figure 10 shows changes in CDD and CWD over the near, mid and far future under RCP4.5 and RCP8.5 scenarios compared to the reference period. The same pattern is observed for CDD under both RCP4.5 and RCP8.5 scenarios. Indeed, a mix of decrease ranging between 10 and 30% and an increase of about 25% is simulated. The increase in CDD is found in the southwest over the three sub-periods. The pattern of CWD under RCP4.5 and RCP8.5 scenarios is quite similar to the one for CDD. A mix of decrease ranging between 5 and 30% and an increase of about 25% is simulated. The increase in CWD is also found in the southwest over the three sub-periods.

Changes in precipitations frequency indices using RCA4 precipitations data

Figure 11 shows changes in R10 and R20 over the near,

mid and far future under RCP4.5 and RCP8.5 scenarios compared to the reference period. Under RCP4.5 scenarios, a decrease of about 20% is simulated in the north, while an increase of 60% is found in the south-east. Under RCP8.5 scenarios, we also notice the same pattern over the near future, whereas in the mid and far future, the study area would experience an increase up to 80% mostly in the south-east. Under RCP4.5 and RCP8.5 scenarios, an increase (up to 120%) is simulated for R20 in the south-east over the investigated sub-periods.

Changes in CDD and CWD by using RCA4 precipitations simulations over the near, mid and far future under RCP4.5 and RCP8.5 scenarios compared to the reference period are shown in Figure 12. Under both RCP4.5 and RCP8.5, a mix of slight increase in CDD (up to 5%) and a decrease (up to 30%) is simulated. The decrease is mostly observed in the north and center of Oueme at Beterou catchment. Regarding CWD, it is under RCP8.5 scenarios that we notice a highest increase (up to 80%) over the far future.

Projected changes in annual precipitations frequency indices over the near, mid and far future under RCP4.5 and RCP8.5 scenarios

Figure 13 shows changes in annual R10 and R20 under RCP 4.5 and RCP 8.5 scenarios and for the different investigated RCM precipitations. R10 shows an increase of 69% (2020s), 62% (2050s) and 64.5% (2080s) under

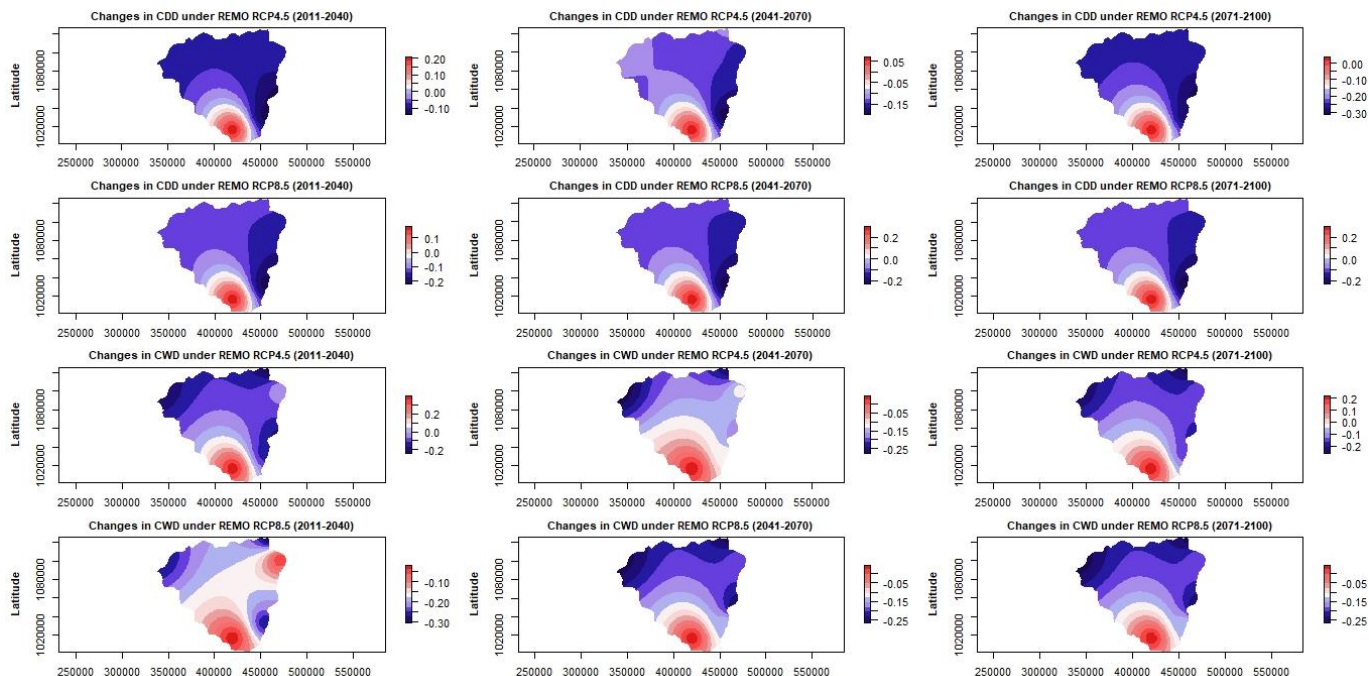


Figure 10. Changes in CDD and CWD using REMO precipitations data.

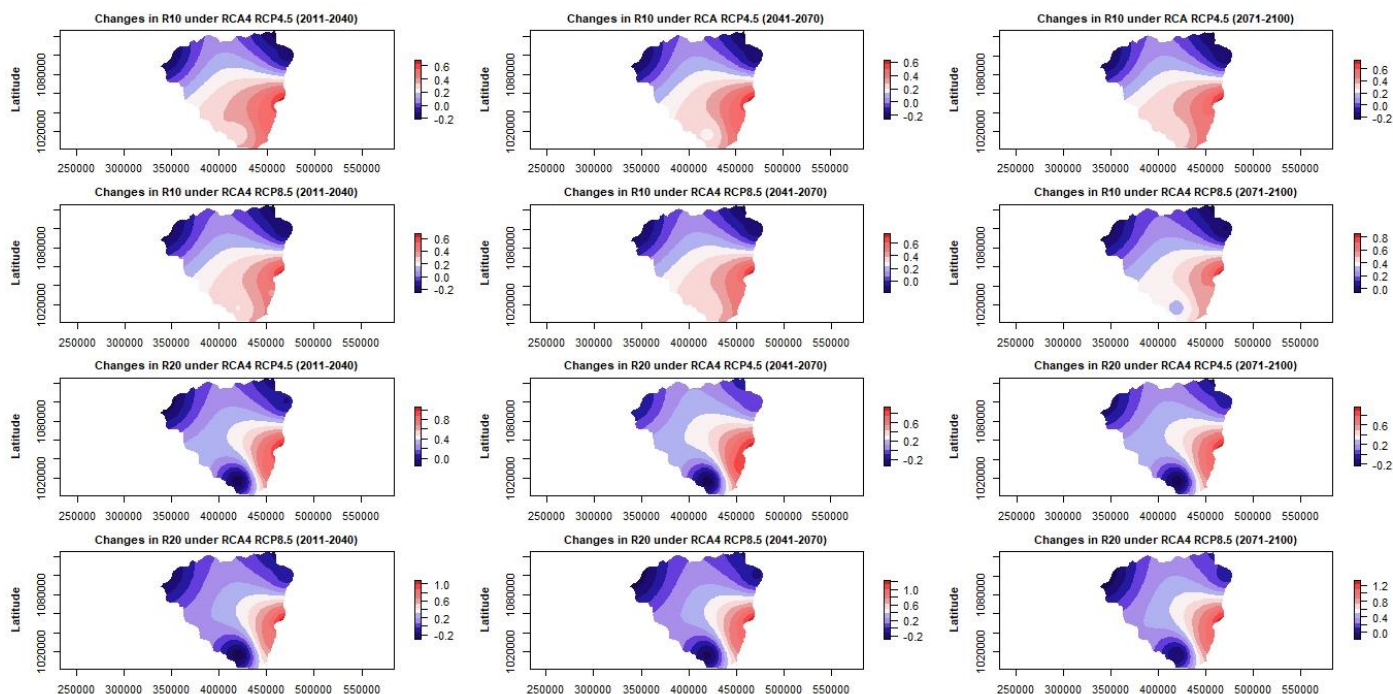


Figure 11. Changes in R10 and R20 using RCA4 precipitations data.

RCP4.5 scenarios, while under RCP8.5 scenarios it will be observed an increase of 65% (2020s), 63% (2050s) and 65% (2080s) with HIRHAM5 simulations. Regarding

REMO simulations, R10 shows an increase of 45% (2020s), 35% (2050s) and 38% (2080s) under RCP4.5 scenarios, while under RCP8.5 scenarios an increase of

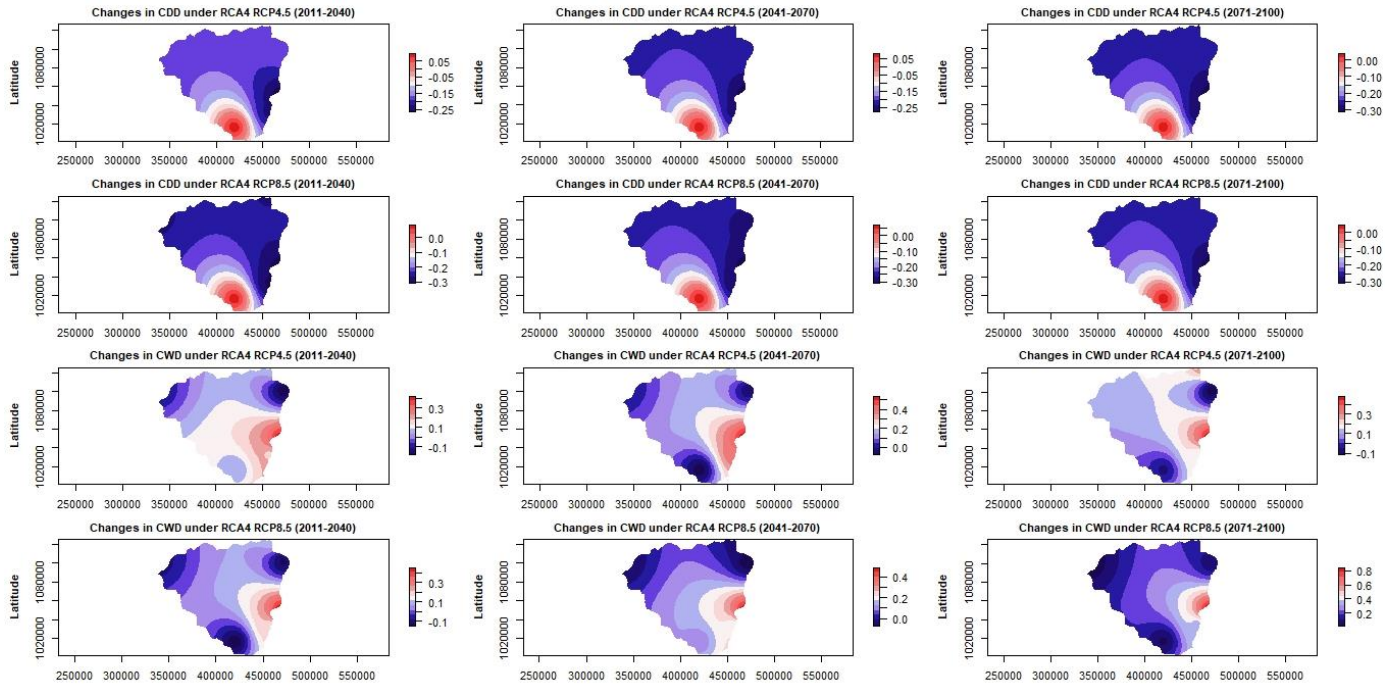


Figure 12. Changes in CDD and CWD using RCA4 precipitations data.

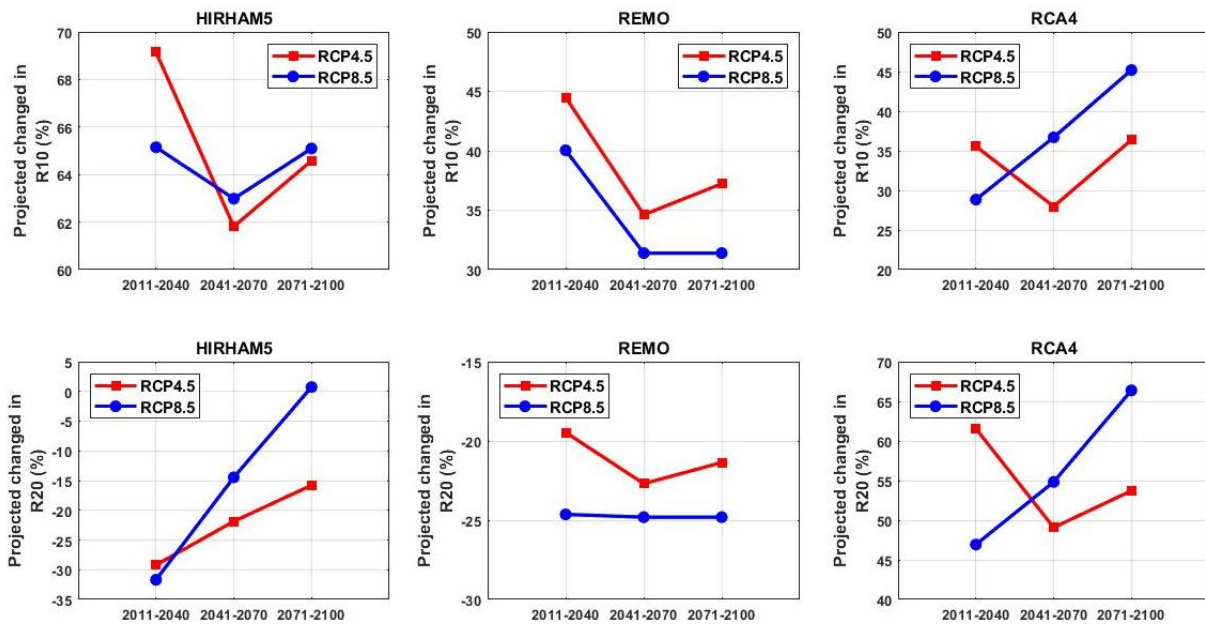


Figure 13. Projected changes in annual R10 and R20 under RCP 4.5 and RCP 8.5 scenarios.

40% (2020s), 31% (2050s and 2080s) could be observed. With RCA4 simulations, R10 shows an increase of 35% (2020s), 28% (2050s) and 37% (2080s) under RCP4.5 scenarios, while under RCP8.5 scenarios an increase of 29% (2020s), 37% (2050s) and 45% (2080s) could be

observed.

R20 shows a decrease of 30% (2020s), 22% (2050s) and 15% (2080s) under RCP4.5 scenarios, while under RCP8.5 scenarios it will be observed a decrease of 32% (2020s), 15% (2050s) and an increase of 1% (2080s)

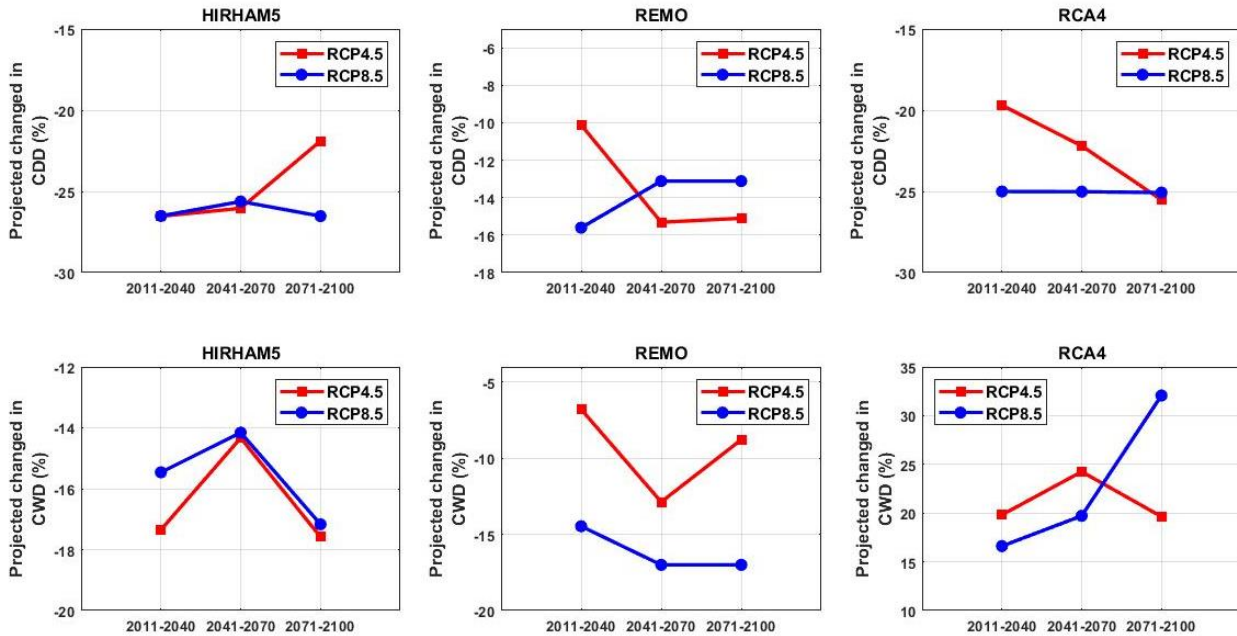


Figure 14. Projected changes in annual CDD and CWD under RCP 4.5 and RCP 8.5 scenarios.

with HIRHAM5 simulations. Regarding REMO simulations, R20 shows a decrease of 18% (2020s), 22% (2050s) and 19% (2080s) under RCP4.5 scenarios, while under RCP8.5 scenarios a decrease of 24% (2020s), 25% (2050s and 2080s) could be observed. With RCA4 simulations, R20 shows an increase of 62% (2020s), 48% (2050s) and 54% (2080s) under RCP4.5 scenarios, while under RCP8.5 scenarios an increase of 47% (2020s), 55% (2050s) and 67% (2080s) could be observed.

Figure 14 shows changes in annual CDD and CWD under RCP 4.5 and RCP 8.5 scenarios and for the different investigated RCM precipitations data. CDD shows a decrease of 27% (2020s), 26% (2050s) and 22% (2080s) under RCP4.5 scenarios, while under RCP8.5 scenarios it will be observed a decrease of 27% (2020s), 27.5% (2050s) and 28% (2080s) with HIRHAM5 simulations. Regarding REMO simulations, CDD shows a decrease of 10% (2020s), 15.5% (2050s) and 15% (2080s) under RCP4.5 scenarios, while under RCP8.5 scenarios a decrease of 16% (2020s), 13% (2050s and 2080s) could be observed. With RCA4 simulations, CDD shows a decrease of 20% (2020s), 22% (2050s) and 26% (2080s) under RCP4.5 scenarios, while under RCP8.5 scenarios a decrease of 25% (2020s, 2050s and 2080s) could be observed.

CWD shows a decrease of 17.5% (2020s), 14% (2050s) and 17.8% (2080s) under RCP4.5 scenarios, while under RCP8.5 scenarios it will be observed a decrease of 15.5% (2020s), 14% (2050s) and 17% (2080s) with HIRHAM5 simulations. Regarding REMO simulations, CWD shows a decrease of 8% (2020s),

12.5% (2050s) and 9% (2080s) under RCP4.5 scenarios, while under RCP8.5 scenarios a decrease of 15% (2020s), 17.5% (2050s and 2080s) could be observed. With RCA4 simulations, CWD shows an increase of 20% (2020s), 25% (2050s) and 20% (2080s) under RCP4.5 scenarios, while under RCP8.5 scenarios an increase of 16% (2020s), 20% (2050s) and 32.5% (2080s) could be observed.

Trends in the extremes precipitations indices

To better capture trends in extremes precipitations indices, averages of the indices were computed by averaging the values of indices over all the stations for the 2020s, 2050s and 2080s under RCP4.5 and RCP8.5 scenarios. Using HIRHAM5 simulations (Table 4), R10 shows statistically increasing trends of order 1.1 days/decade (2020s), 1 days/decade (2050s), 0.9 days/decade (2080s) under both RCP4.5 and RCP8.5 scenarios. R20 shows statistically significant increasing trends of order 0.8 days/decade (2020s) under RCP8.5, around 1.1 days/decade (2050s) under RCP4.5 and RCP8.5 and 1.2 days/decade (2080s) under RCP8.5. CDD and CWD do not show any statistically significant trends. RX5days shows statistically significant increasing trends of order 0.5 mm/decade (2050s) under RCP4.5 and 0.4 mm/decade (2080s) under RCP4.5. SDII shows statistically increasing trends of order 0.3 mm/days/decade (2020s) under RCP4.5 and RCP8.5, 0.3 mm/days/decade (2080s) under RCP4.5 and 0.4 mm/days/decade (2080s) under RCP8.5.

Table 4. Trend analysis of extremes precipitations indices under RCP4.5 and RCP8.5 scenarios with HIRHAM5 simulations.

| Index | 2011 - 2040 | | 2041 - 2070 | | 2071 - 2100 | |
|---------|-------------|---------|-------------|---------|-------------|---------|
| | RCP4.5 | RCP8.5 | RCP4.5 | RCP8.5 | RCP4.5 | RCP8.5 |
| R10 | 0.1174* | 0.1093* | 0.1059* | 0.1125* | 0.0994* | 0.0972* |
| R20 | 0.0847 | 0.0889* | 0.1012* | 0.1114* | 0.105*8 | 0.1240* |
| CDD | 0.0032 | 0.0034 | 0.0001 | -0.0078 | 0.0022 | -0.0018 |
| CWD | 0.00035 | 0.0129 | 0.0056 | -0.0002 | 0.0061 | 0.0065 |
| RX5days | 0.0401 | 0.0293 | 0.0536* | 0.0328 | 0.0443* | 0.0713 |
| SDII | 0.0367* | 0.0342* | 0.0365 | 0.0366 | 0.0362* | 0.0449* |

Numbers in italic represent the significant trends. *Significant at 0.05.

Table 5. Trend analysis of extremes precipitations indices under RCP4.5 and RCP8.5 scenarios with REMO simulations.

| Index | 2011 - 2040 | | 2041 - 2070 | | 2071 - 2100 | |
|--------|-------------|----------|-------------|----------|-------------|----------|
| | RCP4.5 | RCP8.5 | RCP4.5 | RCP8.5 | RCP4.5 | RCP8.5 |
| R10 | 0.0677* | 0.0705* | 0.0724* | 0.0630* | 0.0685* | 0.0630* |
| R20 | 0.0446* | 0.0511 | 0.0429* | 0.0475* | 0.0412* | 0.0475* |
| CDD | -0.0109* | -0.0158* | -0.0152* | -0.0120* | -0.0179* | -0.0120* |
| CWD | *0.0326 | 0.0349* | 0.0335* | 0.0240 | 0.0453* | 0.0240 |
| RX5day | -0.0225 | 0.0100 | -0.0417 | 0.0001 | -0.0303 | 0.0001 |
| SDII | 0.0023 | 0.0132* | -0.0005 | 0.0140 | 0.0003 | 0.0140 |

Numbers in italic represent the significant trends. *Significant at 0.05.

Table 6. Trend analysis of extremes precipitations indices under RCP4.5 and RCP8.5 scenarios with RCA4 simulations.

| Index | 2011 - 2040 | | 2041 - 2070 | | 2071 - 2100 | |
|---------------|-------------|---------|-------------|---------|-------------|---------|
| | RCP4.5 | RCP8.5 | RCP4.5 | RCP8.5 | RCP4.5 | RCP8.5 |
| R10 | 0.1450* | 0.1408* | 0.1386* | 0.1417* | 0.1519* | 0.1338* |
| R20 | 0.2196* | 0.1906 | 0.1951 | 0.2037* | 0.2050 | 0.1868 |
| CDD | -0.0087 | 0.00009 | -0.0054 | -0.0041 | 0.0006 | -0.0022 |
| CWD | 0.0720 | 0.0511 | 0.0407 | 0.0650 | 0.0108 | 0.0428 |
| <i>RX5day</i> | 0.0234 | 0.0232 | 0.0082 | 0.0281 | 0.0155 | 0.0322 |
| <i>SDII</i> | 0.0164 | 0.0225 | 0.0196 | 0.0261 | 0.0220 | 0.0294* |

Numbers in italic represent the significant trends. *Significant at 0.05.

With REMO simulations (Table 5), R10 shows statistically increasing trends of order around 0.7 days/decade (2020s, 2050s and 2080s) under both RCP4.5 and RCP8.5 scenarios. R20 shows statistically significant increasing trends of order 0.4 days/decade (2020s) under RCP4.5, around 0.4 days/decade (2050s and 2080s) under RCP4.5 and RCP8.5. CDD shows statistically decreasing trends of order 0.1 days/decade (2020s, 2040s and 2080s) under RCP4.5 and RCP8.5. CWD shows statistically significant increasing trends of order 0.3 days/decade (2020s) under RCP4.5 and RCP8.5, 0.3 days/decade (2050s) under RCP4.5 and 0.4 days/decade (2080s) under RCP4.5. RX5days do not show any

statistically significant trends. SDII shows only a slight statistically significant increasing trend of order 0.1 mm/days/decade (2020s) under RCP8.5.

Regarding RCA4 simulations (Table 6), R10 shows statistically increasing trends of order around 1.4 days/decade (2020s, 2050s and 2080s) under both RCP4.5 and RCP8.5. R20 shows statistically significant increasing trends of order 0.2 days/decade (2020s) under RCP4.5, 0.2 days/decade (2050s) under RCP8.5. CDD, CWD and RX5days do not show any statistically significant trends. SDII shows only a slight statistically significant increasing trend of order 0.2 mm/days/decade (2080s) under RCP8.5 scenario.

DISCUSSION

Understanding the changes in the intensity and frequency of extreme precipitation is crucial for flood risk mitigation and water resource management in the studied area. This paper presents an overview of future changes in extreme precipitation indices in the Ouémé River basin at Beterou. We compare the changes in extreme precipitation over the 2020s, 2050s, and 2080s under RCP4.5 and RCP8.5 scenarios to the reference period (1961-1990). The ISIMIP bias correction method is utilized to bias correct precipitation data before computing the extreme indices. Several studies have demonstrated that the ISIMIP method is one of the best bias correction methods (Obada et al., 2016; Wörner et al., 2019).

The impacts of climate change on precipitation extremes in the studied area have been established. The results indicate an increase in changes in almost all precipitation intensity (RX5days and SDII) and frequency indices (R10, R20, CDD, and CWD) compared to the reference period over the 2020s, 2050s, and 2080s under RCP4.5 and RCP8.5 scenarios. The increasing rate is comparatively higher under the RCP8.5 scenarios, mostly in the mid and far future. Similar results have also been found by Allechy et al. (2022) using CHIRPS data and data from 4 GCM (CanESM2, HadGEM2-ES, MIROC-ESM, and MIROC-ESM-CHEM) in the Lobo river catchment in Cote d'Ivoire. Although the observed changes in extreme precipitation indices are consistent across various data sources and the available literature, one key issue are the magnitudes of such recent changes, which vary considerably between different data sources (Sylla et al., 2016).

The results show almost statistically significant increasing trends in precipitation intensity and frequency indices. These results support the findings of earlier studies on severe precipitation indices in various regions. Positive trends in RX5Day and CDD, and negative trends in consecutive wet days (CWD), are consistent with those reported in East Africa and Ethiopia by Mohamed et al. (2022), Central Africa (Sonkoué et al., 2019), West Africa (Tamoffo et al., 2023; Amichiatchi et al., 2024), Southern Africa (Samuel et al., 2023), over the Mediterranean and Sahara regions (Babaousmail et al., 2022), and in Asia (Ashesh and Rajib, 2023). The increasing trends in extreme precipitation intensity and frequency might lead to more floods in the Ouémé River basin at Beterou (Deng et al., 2018). Gamal et al. (2024) also highlighted that the expected increases in the severity and frequency of climatic extremes (droughts and floods) have a significant impact on the region's food, water security status, and natural environment. Indeed, the increase in all the wet indices over the studied area would lead to the intensification of the hydrological cycle, which could increase the frequency and intensity of floods in the future. Such significant information is useful for farmers and decision-makers to ensure the survival and

prosperity of the population.

Many studies have investigated the potential causes of extreme precipitation changes over West Africa (Diatta et al., 2020; Atiah et al., 2020; Ta, 2016; Ahokpossi, 2019). They concluded that West African extreme precipitation is highly influenced by large-scale ocean surface temperatures and atmospheric conditions in the tropical Atlantic. Ta (2016) found that extreme precipitation on the Guinean coast is greatly associated with Atlantic sea surface temperature (SST) anomalies, the Northern Cold Tongue Index, and with an opposite sign of Nino3.4. Over Benin, the North Atlantic Oscillation, Pacific Decadal Oscillation, and Nino3 negatively influence precipitation, while the Southern Oscillation, Antarctic Oscillation, and Dipole Mode Index positively correlate with precipitation (Ahokpossi, 2019).

Conclusions

The primary contribution of this paper was to assess future changes in extreme precipitation indices compared to the reference period. The ISIMIP bias correction method utilized in this study helps reduce the significant differences between observed data and RCM simulations. Under both RCP4.5 and RCP8.5 scenarios, the results indicate a combination of increases and decreases in precipitation intensity indices, ranging between -40 and 40% with HIRHAM5 and RCA4, while REMO only shows increases ranging from 2 to 80% across the three time horizons: 2020s, 2050s, and 2080s. Regarding precipitation frequency indices, there is also a mix of increases and decreases, ranging between -40 and 80%, across the three time horizons under both RCP4.5 and RCP8.5 scenarios using HIRHAM5, REMO, and RCA4 precipitations. This study lays the groundwork for water management and further adaptations to climate change. The insights gleaned from this study will be valuable for farmers and decision-makers in ensuring the survival and prosperity of the population.

CONFLICT OF INTERESTS

The authors have not declared any conflict of interests.

ACKNOWLEDGEMENT

The authors are grateful for the funding and support given by the International Foundation for Science (IFS) under IFS grant No. I2-W-6600-1.

REFERENCES

Ahokpossi Y (2019). Analysis of the rainfall variability and change in the Republic of Benin (West Africa). *Hydrological sciences Journal* 63(15-16):2097-2123.

- Alamou EA, Zandagba JE, Biao EI, Obada E, Da-Allada CY, Bonou FK, Pomalegni Y, Baloitcha E, Tilmes S, Irvine PJ (2022). Impact of stratospheric aerosol geoengineering on extreme precipitation and temperature indices in West Africa using GLENS simulations. *Journal of Geophysical Research: Atmospheres* 127(9):e2021JD035855 <https://doi.org/10.1029/2021JD035855>.
- Allechy FB, Youan TaM, N'guessan Bi VH, Yapi AF, Kouakou JRE, Affian K (2022). Évolution passée et future des précipitations extrêmes dans le Centre-Ouest de la Côte d'Ivoire: cas du bassin versant de la rivière Lobo Résumé 20(1):93-111.
- Amichiatchi NJMC, Hounkpè J, Soroc GE Khadijata OO, Larbid I, Limantold AM, Alhassand ARM, Goula BTA, Lawin AE (2024). Analysis of past and projected changes in extreme precipitation indices in some watersheds in Côte d'Ivoire, *Journal of Water and Climate Change* 15(2):392. doi: 10.2166/wcc.2023.365.
- Ahsan S, Bhat MS, Alam A, Farooq H, Shiekh HA (2021). Evaluating the impact of climate change on extreme temperature and precipitation events over the Kashmir Himalaya, *Climate Dynamics* 58:1651-1669. Available at: <https://doi.org/10.1007/s00382-021-05984-6>.
- Paul AR, Maity R (2023). Future projection of climate extremes across contiguous northeast India and Bangladesh. *Scientific Reports* 13(1):15616.
- Atiah WA, Mengistu TG, Amekudzi LK, Yorke C (2020). Trends and interannual variability of extreme rainfall indices over Ghana, West Africa. *Theoretical and Applied Climatology* 140:1393-1407.
- Avila-Diaz A, Benezoli V, Justino F, Torres R, Wilson A (2020). Assessing current and future trends of climate extremes across Brazil based on reanalyses and earth system model projections. *Climate Dynamics* 55(5):1403-1426. Available at: <https://doi.org/10.1007/s00382-020-05272-9>.
- Baboumail H, Hou R, Ayugi B, Sian KTCLK, Ojara M, Mumo R, Ongoma V (2022). Future changes in mean and extreme precipitation over the Mediterranean and Sahara regions using bias-corrected CMIP6 models. *International Journal of Climatology* 42(14):7280-7297.
- Ceron WL, Kayano MT, Andreoli RV, Avila-Diaz A, Ayes I, Freitas ED, Martins JA, Souza RAF (2021). Recent intensification of extreme precipitation events in the La Plata basin in southern South America (1981-2018). *Atmospheric Research* 249:105299. Available at: <https://doi.org/10.1016/j.atmosres.2020.105299>.
- Christensen JH, Hewitson B, Busiuc A, Chen A, Gao X, co-authors (2007). Regional climate projections. In: *Climate Change: The Physical Science Basis. Contribution of Working Group I to the Fourth Assessment Report of the Intergovernmental Panel on Climate Change* (eds S. Solomon D, Qin M, Manning Z, Chen M, Marquis and co-editors). Cambridge University Press, Cambridge, United Kingdom and New York, NY, USA.
- Christensen OB, Drews M, Christensen JH (2017). The HIRHAM regional climate model version P 5. Available at: http://orbit.dtu.dk/fedora/objects/orbit:118724/datastreams/file_8c69af6e-acfb-4d1aaa53-73188c001d36/content.
- Deng Y, Jiang W, He B, Chen Z, Jia K (2018). Change in intensity and frequency of extreme precipitation and its possible teleconnection with large-scale climate index over the China from 1960 to 2015. *Journal of Geophysical Research: Atmospheres* 123(4):2068-2081. Available at: <https://doi.org/10.1002/2017JD027078>.
- Diatta S, Diedhiou CW, Dione DM, Sambou S (2020). Spatial variation and trend of extreme precipitation in West Africa and teleconnections with remote indices. *Atmosphere* 11(9):999.
- Donat MG, Lowry AL, Alexander LV, O'Gorman PA, Maher N (2016). More extreme precipitation in the world's dry and wet regions. *Nature Climate Change* 6(5):508-513.
- Faye A, Akinsanola AA (2022). Evaluation of extreme precipitation indices over West Africa in CMIP6 models. *Climate Dynamics* 58(3):925-939. <https://doi.org/10.1007/s00382-021-05942-2>.
- Gamal G, Nejedlik P, El Kenawy AM (2024). Assessing Future Precipitation Patterns, Extremes and Variability in Major Nile Basin Cities: An Ensemble Approach with CORDEX CORE Regional Climate Models. *Climate* 12(1):9. Available at: <https://doi.org/10.3390/cli12010009>.
- Gouveia CD, Torres RR, Marengo JA, Avila-Diaz A (2022). Uncertainties in projections of climate extremes in South America via Bayesian inference. *International Journal of Climatology* 42(14):7362-7382. Available at: <https://doi.org/10.1002/joc.7650>.
- Haylock MR, Cawley GC, Harpham C, Wilby RL, Goodess CM (2006). Downscaling heavy precipitation over the United Kingdom: A comparison of dynamical and statistical methods and their future scenarios. *International Journal of Climatology: A Journal of the Royal Meteorological Society* 26(10):1397-1415.
- Intergovernmental Panel on Climate Change (IPCC) (2007). *Climate Change 2007—Synthesis Report*. Intergovernmental Panel on Climate Change. Cambridge University Press: Cambridge, UK.
- Intergovernmental Panel on Climate Change (IPCC) (2014). *Climate Change 2014: Impacts, Adaptation, and Vulnerability. Part A: Global and Sectoral Aspects. Contribution of Working Group II to the Fifth Assessment Report of the Intergovernmental Panel on Climate Change* [Field CB, Barros VR, Dokken DJ, Mach KJ, Mastrandrea MD, Bilir TE, Chatterjee M, Ebik L, Estrada YO, Genova RC, Girma B, Kissel ES, Levy AN, MacCracken S, Mastrandrea PR, White LL (Eds.)]. Cambridge University Press, Cambridge, United Kingdom and New York, NY, USA 1132 p.
- Jacob D, Bärring L, Christensen OB, Christensen JH, de Castro M, Déqué M, Giorgi F, Hagemann S, Hirschi M, Jones R, Kjellström E, (2007). An inter-comparison of regional climate models for Europe: model performance in present-day climate. *Climatic change* 81:31-52.
- Kharin VV, Zwiers FW, Zhang X, Wehner M (2013). Changes in temperature and precipitation extremes in the CMIP5 ensemble. *Clim Change* 119(2):345-357. Available at: <https://doi.org/10.1175/JCLI4066.1>.
- Lacovone MF, Pantano VC, Penalba OC (2020). Consecutive dry and wet days over South America and their association with enso, in cmip5 simulations. *Theor. Appl. Climatol.* 142:791-804. Available at: <https://doi.org/10.1007/s00704-020-03324-y>.
- Lawin AE (2007). Analyse climatologique et statistique du régime pluviométrique de la haute Vallée de l'Ouémé à partir des données pluviographiques AMMA-CATCH-Bénin. Thèse de doctorat, Institut National Polytechnique de Grenoble P 221.
- Le Lay M (2006). Modélisation hydrologique dans un contexte de variabilité hydro-climatique. Une approche comparative pour l'étude du cycle hydrologique à méso-échelle au Bénin. Thèse de Doctorat, France: Institut National Polytechnique de Grenoble-INPG P 67.
- Mohammed JA, Gashaw T, Tefera GW, Dile YT, Worqlul AW, Addisu S. (2022). Changes in observed rainfall and temperature extremes in the Upper Blue Nile Basin of Ethiopia. *Weather and Climate Extremes* 37:100468.
- Obada E, Alamou AE, Zandagba EJ, Biao IE, Chabi A, Afouda A (2016). Comparative study of seven bias correction methods applied to three Regional Climate Models in Mekrou catchment (Benin, West Africa).
- Orlowsky B, Seneviratne SI (2012). Global changes in extreme events: regional and seasonal dimension. *Climatic change* 110(3-4):669-696. Available at: <https://doi.org/10.1007/s10584-011-0122-9>.
- Paeth H (2011). Postprocessing of Simulated Precipitation for Impact Research in West Africa. Part I: Model Output Statistics for Monthly Data. *Climate Dynamics* 36:1321-1336. Available at: <http://dx.doi.org/10.1007/s00382-010-0760-z>.
- Regoto P, Dereczynski C, Chou SC, Bazzanella AC (2021). Observed changes in air temperature and precipitation extremes over Brazil. *International Journal of Climatology* 41(11):5125-5142. Available at: <https://doi.org/10.1002/joc.7119>.
- Samuel S, Dosio A, Mphale K, Faka DN, Wiston M (2023). Comparison of multimodel ensembles of global and regional climate models projections for extreme precipitation over four major river basins in southern Africa—Assessment of the historical simulations. *Climatic Change* 176(5):57.
- Samuelsson P, Jones CG, Wille'n U, Ullerstig A, Gollvik S, Hansson U, Kjellström E, Nikulin G, Wyser K (2011). The Rossby Centre regional climate model RCA3: model description and performance. *Tellus A: Dynamic Meteorology and Oceanography* 63(1):4-23.
- Sen PK (1968). Estimates of the Regression Coefficient Based on Kendall's Tau. *Journal of the American statistical association* 63(324):1379-1389.

- Sillmann J, Roeckner E (2008). Indices for extreme events in projections of anthropogenic climate change. *Climate Change* 86(1-2):83-104. Available at: <https://doi.org/10.1007/s10584-007-9308-6>.
- Sillmann J, KharinVV, Zwiers FW, Zhang X, Bronaugh D (2013). Climate extremes indices in the CMIP5 multimodel ensemble: Part 2. Future climate projections. *Journal of geophysical research: atmospheres* 118(6):2473-2493. Available at: <https://doi.org/10.1002/jgrd.50188>.
- Sonkoué D, Monkam D, Fotso-Nguemo TC, Yepdo ZD, Vondou DA (2019). Evaluation and projected changes in daily rainfall characteristics over Central Africa based on a multi-model ensemble mean of CMIP5 simulations. *Theoretical and Applied Climatology* 137:2167-2186.
- Sultan B, Gaetani M (2016). Agriculture in West Africa in the twenty-first century: Climate change and impacts scenarios, and potential for adaptation. *Frontiers in plant science* 7:211434. Available at: <https://doi.org/10.3389/fpls.2016.01262>.
- Sylla MB, Elguindi N, Giorgi F, Wisser D (2016). Projected robust shift of climate zones over West Africa in response to anthropogenic climate change for the late 21st century. *Climatic Change* 134(1):241-253.
- Ta S, Kouadio KY, Ali KE, Toualy E, Aman A, Yoroba F (2016). West Africa extreme rainfall events and large-scale ocean surface and atmospheric conditions in the Tropical Atlantic. *Advanced in Meteorology* 1:1-16.
- Tamoffo AT, Weber T, Akinsanola AA, Vondou DA (2023). Projected changes in extreme rainfall and temperature events and possible implications for Cameroon's socio-economic sectors. *Meteorological Applications* 30(2):e2119.
- Thibeault JM, Seth A (2014). Changing climate extremes in the Northeast United States: observations and projections from CMIP5. *Climatic change* 127(2014):273-287. Available at: <https://doi.org/10.1007/s10584-014-1257>.
- Wörner V, Kreye P, Meon G (2019). Effects of bias-correcting climate model data on the projection of future changes in high flows. *Hydrology* 6(2):46. Available at: <https://doi.org/10.3390/hydrology6020046>.
- Xu K, Xu B, JuJ, Wu C, Dai H, Hu BX (2019). Projection and uncertainty of precipitation extremes in the CMIP5 multimodel ensembles over nine major basins in China. *Atmospheric Research* 226:122-137. Available at: <https://doi.org/10.1016/j.atmosres.2019.04.018>.
- Yang W, Andreasson J, Graham LP, Olsson J, Rosberg J, Wetterhall F (2010). Distribution-based scaling to improve usability of regional climate model projections for hydrological climate change impacts studies. *Hydrology Research* 41(3-4):211-229.
- Zhang X, Alexander L, Hegerl GC, Jones P, Tank AK, Peterson TC, Trewin B, Zwiers FW (2011). Indices for monitoring changes in extremes based on daily temperature and precipitation data, *WIREs. Climate Change* 2(6):851-870.